



# Mitochondrial permeability transition as a novel principle of hepatorenal toxicity *in vivo*

D. Haouzi, I. Cohen, H. L. A. Vieira, D. Poncet, P. Boya, M. Castedo, N. Vadrot, A.-S. Belzacq, D. Fau, C. Brenner, G. Feldmann and G. Kroemer

Centre National de la Recherche Scientifique, UMR1599, Institut Gustave Roussy, 39 rue Camille-Desmoulins, F-94805 Villejuif, France (D. Haouzi, I. Cohen, H. L. A. Vieira, D. Poncet, P. Boya, M. Castedo, C. Brenner, G. Kroemer); Institut National pour la Santé et pour la Recherche Médicale, U327, Faculté de Médecine Xavier Bichat, 16 rue Henri Huchard, F-75018 Paris, France (N. Vadrot, G. Feldmann); Centre National de la Recherche Scientifique, UMR6022, Université de Technologie de Compiègne, BP 20529, F-60205 Compiègne, France (A.-S. Belzacq, C. Brenner); Centre National de la Recherche Scientifique, FRE2174, Faculté de Médecine et de Pharmacie Saint Jacques, F-25039 Besançon, France (D. Fau)

**Atractyloside (Atr) binds to the adenine nucleotide translocator (ANT) and inhibits ANT-mediated ATP/ADP exchange on the inner mitochondrial membrane. In addition, Atr can trigger opening of a non-specific ion channel, within the ANT-containing permeability transition pore complex (PTPC), which is subject to redox regulation and inhibited by cyclosporin A (CsA). Here we show that the cytotoxic effects of Atr, both *in vivo* and *in vitro*, are determined by its capacity to induce PTPC opening and consequent mitochondrial membrane permeabilization (MMP). Thus, the Atr-induced MMP and death of cultured liver cells are both inhibited by CsA as well as by glutathione (GSH) and enhanced by GSH depletion. Similarly, the hepatorenal toxicity of Atr, assessed *in vivo*, was reduced by treating mice with CsA or a diet rich in sulfur amino acids, a regime which enhances mitochondrial GSH levels. Atr injection induced MMP in hepatocytes and proximal renal tubular cells, and MMP was reduced by either CsA or GSH. Acetaminophen (paracetamol)-induced acute poisoning was also attenuated by CsA and GSH, both *in vitro* and *in vivo*. Altogether these data indicate that PTPC-mediated MMP may determine the hepatorenal toxicity of xenobiotics *in vivo*.**

**Keywords:** adenine nucleotide translocator; apoptosis; bax, cell death; mitochondria.

## Introduction

The diterpenoid glycoside atractyloside (Atr) and its derivative carboxyatractyloside are the principal toxic compounds contained in several plants, namely *Atractylis gommifera* (the most frequent causative agent of acute

herbal poisoning, mainly of children, in Mediterranean countries), *Callipepis laureola* (a traditional remedy used in South Africa),<sup>1</sup> and *Xanthium strumarium* (cocklebur, a plant grazed by cattle).<sup>2</sup> Oral ingestion of Atr causes fatal renal proximal tubule necrosis and/or centrilobular hepatic necrosis. The specificity of this Atr effect may be attributed to the selective capacity of proximal tubular epithelial cells and hepatocytes to enrich the hydrophilic (normally plasma membrane impermeable) Atr molecule via active transport.<sup>3,4</sup> Atr specifically interacts with a mitochondrial protein, the adenine nucleotide translocator (ANT),<sup>5</sup> in a fashion that is modulated by the thiol oxidation state of ANT.<sup>6–8</sup>

ANT is a bifunctional protein contained in the inner mitochondrial membrane.<sup>9</sup> On the one hand, ANT is responsible for the exchange (antiport) of ATP and ADP on the inner mitochondrial membrane, a function that is essential for fueling ATP generated through oxidative phosphorylation to the extramitochondrial compartments.<sup>10</sup> On the other hand, ANT forms part of the permeability transition pore complex (PTPC),<sup>11</sup> a multiprotein complex in which ANT interacts with the voltage dependent anion channel (VDAC, in the outer membrane), cyclophilin D (in the mitochondrial matrix), as well as members of the apoptosis-regulatory Bcl-2/Bax family.<sup>11–18</sup> In the context of the PTPC, ANT can form a non-specific pore<sup>9,13,19–21</sup> whose opening results in mitochondrial membrane permeabilization (MMP), an event that participates both in apoptotic and necrotic cell death.<sup>17,18,22</sup> Formation of ANT pores is stimulated by Ca<sup>2+</sup>,<sup>19,20</sup> Bax,<sup>13,21,23,24</sup> thiol oxidation,<sup>8</sup> nitric oxide, reactive oxygen species,<sup>25</sup> as well as by some chemotherapeutic agents.<sup>26</sup>

Atr is known to have two effects on ANT. On the one hand, Atr can inhibit the ATP/ADP antiporter function of ANT,<sup>27</sup> and this property of Atr has been taken advantage

Correspondence to: Dr. Guido Kroemer, CNRS-UMR1599, Institut Gustave Roussy, Pavillon de Recherche 1, 39 rue Camille-Desmoulins, F-94805 Villejuif, France. Tel: 33-1-42 11 6046; Fax: 33-1-42 11 6047; e-mail: kroemer@igr.fr

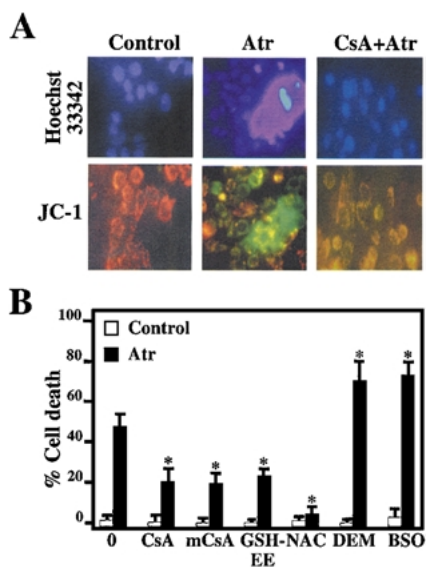
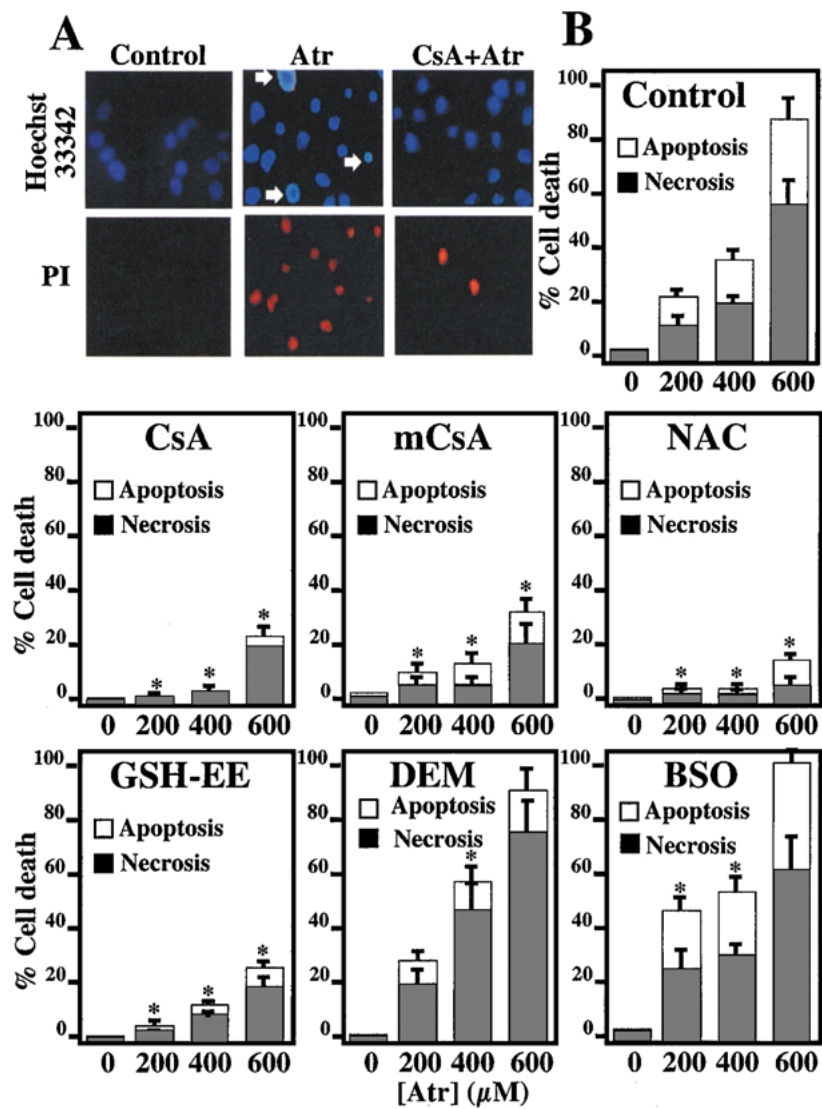


**Figure 2.** Atr-induced  $\Delta\Psi_m$  dissipation in liver cells. (A) Atr-induced shift in the JC-1 emission spectrum. Liver cells were exposed to 600  $\mu\text{M}$  Atr for 2 h (preceded by pre-incubation with CsA as in Figure 1A) and cells were stained with the  $\Delta\Psi_m$ -sensitive dye JC-1. Note the red-green shift in JC-1 fluorescence induced by Atr. CsA largely prevented this shift. The orange and red cells were considered as  $\Delta\Psi_m^{\text{high}}$ , while cells exhibiting a diffuse green fluorescence were scored as  $\Delta\Psi_m^{\text{low}}$ . (B) Cells were first treated with cyclophilin D ligands (CsA, m-CsA), GSH precursors (NAC, GSH ethyl ester), or GSH-depleting agents (DEM, BSO) and then cultured for 2 hours in the absence (control) or presence of Atr (400  $\mu\text{M}$ ), followed by JC-1 staining as in A. Asterisks denote significant ( $p < 0.01$ ) differences as compared to Atr-only treated cells.

**Figure 1.** Atr-mediated hepatotoxicity *in vitro*. (A) Atr-induced apoptosis and necrosis. Human liver cells were cultured in the absence (control) or presence of Atr (600  $\mu\text{M}$ , 2 h), followed by vital staining with propidium iodine (PI, red fluorescence) plus Hoechst 33342 (blue fluorescence) and fluorescence microscopic inspection. Cells incorporating PI without chromatin condensation were scored as "necrotic" and cells showing chromatin condensation were scored as "apoptotic" (arrows). Pretreatment with CsA (10  $\mu\text{M}$ , 30 min) resulted in a significant inhibition of cell death. (B) Quantitative assessment of Atr toxicity and its modulation by cyclophilin D ligands (CsA, m-CsA), GSH precursors (NAC, GSH ethyl ester), or GSH-depleting agents (DEM, BSO) and the frequency of necrotic and apoptotic cells was scored as in A. Results are means of four experiments  $\pm$  SEM. Asterisks denote significant ( $p < 0.01$ , paired Student t test) differences with respect to Atr-only treated cells.

of to study the contribution of ANT to the control of oxidative phosphorylation. In addition, when added to purified mitochondria *in vitro*, Atr induces the permeability transition (PT),<sup>28,29</sup> that is the partial permeabilization of the inner mitochondrial membrane (to solutes up to 1500 Da), coupled to the complete permeabilization of the outer membrane, resulting in the release of soluble intermembrane proteins including the caspase activator cytochrome *c*,<sup>30,31</sup> mitochondrial pro-caspases,<sup>31,32</sup> and the caspase-independent death effector apoptosis inducing factor (AIF).<sup>33</sup> The Atr-induced PT (but not the inhibition of ANT-mediated antiport) is counteracted by cyclosporin A (CsA),<sup>28</sup> presumably through the inhibition of the interaction between ANT and cyclophilin D (the mitochondrial CsA target) which favors the assembly of the PTPC.<sup>7,14,15,17</sup>

Most studies on the cytotoxic effects of Atr have been performed in cell-free systems<sup>30–32,34,35</sup> or in a rather artificial setting, for instance by microinjection of Atr into cell lines,<sup>13</sup> or by adding Atr to precision-cut rat kidney and liver slices.<sup>4</sup> Here, we studied the cytotoxic effect of Atr on human hepatoma cell lines, *in vitro*. Having found that glutathione GSH and CsA potently inhibit cytotoxic Atr effects *in vitro* we evaluated the effects of dietary cysteine (one of the rate-limiting precursors of GSH) and CsA *in vivo*, in a mouse model of Atr toxicity. Our data reveal that the toxic effects of Atr can be attributed to its capacity to trigger MMP *in vivo*, in liver and proximal renal tubular cells. CsA and a diet rich in sulfur amino acids (SAA) counteract the Atr effect *in vivo*, in the living organism. Stimulated by this precedent, we also show that the acute hepatocellular toxicity of acetaminophen is strongly reduced by CsA medication, suggesting that MMP-induction may be indeed a novel principle of *in vivo* toxicity.

## Materials and methods

### Animals and *in vivo* treatments

Male adult CR1:CD1-ICR BR Swiss mice (30 to 32 g body weight) were obtained from Charles River (Saint-Aubin-Les-Elbeufs, France). Mice were allowed water and food ad libitum and were fed either on a standard diet (A04-biscuits) or on a sulfur amino acid deficient (SAA<sup>-</sup>) or sulfur amino acid-enriched (SAA<sup>+</sup>) diet for 4 and 2 weeks,

respectively, as described.<sup>36</sup> This diet enhances or reduces the concentration of mitochondrial GSH in liver cells by 34 and 58%, respectively, when GSH levels were determined in isolated mitochondria.<sup>37</sup> Mice were injected intraperitoneally (i.p.) with Atr sodium salt (Atr, 300 mg/kg in 100  $\mu\text{l}$  PBS, Sigma, St. Louis, MO) or acetaminophen (600 mg/kg in 50  $\mu\text{l}$  50% ethanol, Sigma). Where indicated, mice were pretreated with cyclosporin A (CsA, Sigma), administered either by intraperitoneal injection (100 mg/kg, in 50  $\mu\text{l}$  50% ethanol 1 hour before Atr) or by means of an osmotic pump (Alzet model 1003D, Durect Co, Cupertino, CA) loaded with 100 mg CsA in 100  $\mu\text{l}$  25% ethanol, implanted subcutaneously (20 hours before acetaminophen; release of 1 mg CsA per hour). Histological (hematoxylin/eosin) and ultrastructural (uranyl acetate/lead citrate) analyses were performed as described.<sup>38</sup>

### Cell lines and apoptosis induction

The human hepatic cell line WRL-68 was cultured in EMEM (Sigma) supplemented with 2 mM glutamine, 1% non-essential amino acids and 10% fetal bovine serum at 37°C under 5% CO<sub>2</sub>. To induce death, cells (2  $\times$  10<sup>5</sup>/ml) were cultured in the presence of Atr (200, 400, or 600  $\mu\text{M}$ ), or acetaminophen (20 mM), for 2 hours. For cell death modulation, cyclosporin A (CsA, 10  $\mu\text{M}$ ), N-methyl-4-Val-CsA (mCsA, 1  $\mu\text{M}$ , SDZ 220-384; kindly provided by Dr. Roland Wenger, Novartis, Basel, Switzerland), NAC (50  $\mu\text{M}$ , Sigma), GSH ethyl ester (10 mM), BSO (0.2 mM) or DEM (0.25 mM) were added 30 minutes (for each modulator except BSO) or 20 hours (for BSO) before adding Atr, or acetaminophen.

### Assessment of apoptosis-associated parameters

Cells cultured on a cover slip were stained with 5,5',6,6'-tetrachloro-1,1', 3,3'-tetraethylbenzimidazolylcarbocyanine iodide (JC-1, 3  $\mu\text{M}$ , Molecular Probes) and Hoechst 33342 (2  $\mu\text{M}$ , Sigma), or propidium iodine (1  $\mu\text{M}$ ) and Hoechst 33342, followed by fluorescence microscopic assessment of apoptotic parameters, as described.<sup>39,40</sup> Paraffin-embedded tissue sections were deparaffinized and stained for the detection of cytochrome *c* (mouse monoclonal antibody 556432 from Pharmingen, detected by

an anti-mouse IgG conjugated with phycoerythrin, PE), cytochrome *c* oxidase (anti-COX subunit IV 20E8-C12 mouse monoclonal from Molecular Probes, detected by a goat anti-mouse IgG conjugated with FITC), AIF (anti-AIF rabbit polyclonal antibody,<sup>33</sup> detected by a goat anti-rabbit IgG conjugated with FITC), or heat shock protein Hsp 60 (mouse anti-Hsp 60 IgG1 antibody H4149 from Sigma, detected by an anti-mouse IgG1 conjugated with PE).<sup>39,40</sup>

### Purification of ANT and its reconstitution into liposomes

Rat heart mitochondria were isolated for ANT purification. After mechanical shearing, mitochondria were suspended in 220 mM mannitol, 70 mM sucrose, 10 mM HEPES, 200  $\mu$ M EDTA, 100 mM DTT, 0.5 mg/ml subtilisin (Sigma), pH 7.4, kept 8 min on ice and sedimented twice by differential centrifugations (5 min, 500  $\times$  g and 10 min, 10,000  $\times$  g). Mitochondrial proteins were solubilized by 6% [v:v] Triton X-100 (Boehringer Mannheim) in 40 mM  $K_2HPO_4$ , 40 mM KCl, 2 mM EDTA, pH 6.0, for 6 min at RT and solubilized proteins were recovered by ultracentrifugation (30 min, 24,000  $\times$  g, 4°C). Then, the Triton X-100 extract was applied to a column filled with 1 g of hydroxyapatite (BioGel HTP, BioRad), eluted with the previous buffer and diluted [v:v] with 20 mM MES (2-[*N*-morpholino]ethanesulfonic acid), 200  $\mu$ M EDTA, 0.5% Triton X-100, pH 6.0. Subsequently, the sample was separated on a Hitrap SP column using a FPLC system (Pharmacia) and a linear NaCl gradient (0–1 M).<sup>8,13</sup> Purified ANT was reconstituted in phosphatidylcholine/cardiophilin liposomes. For liposome preparation, 90 mg phosphatidylcholine and 2 mg cardiophilin were mixed in 1 ml chloroform, and the solvent was evaporated under nitrogen. Dry lipids were resuspended in 1 ml liposomes buffer (125 mM sucrose, 10 mM HEPES) containing 0.3% *n*-octyl- $\beta$ -D-pyranoside and mixed by continuous vortexing for 40 min at RT. ANT (0.1 mg/ml) was then mixed with liposomes [v:v] and incubated for 15 min at RT. ANT proteoliposomes were finally dialyzed overnight at 4°C. Plain liposomes were produced for control tests.<sup>9</sup>

### Quantification of liposomal permeabilization

Plain liposomes and ANT proteoliposomes were sonicated in the presence of 4-umbelliferylphosphate (4-MUP, 1 mM, Sigma) and 10 mM KCl (50 W, 22 sec, Branson sonifier 250) on ice and washed on Sephadex G-25 columns (PD-10, Pharmacia). 25  $\mu$ l-aliquots of liposomes were mixed [v:v] with Atr sodium salt at 100  $\mu$ M, and incubated for 1 h at RT and diluted to 200  $\mu$ l in liposome buffer. In some experiments, liposomes were pre-

treated with CsA (10  $\mu$ M), ATP (1 mM), GSH (500  $\mu$ M, 20 min before Atr) and/or GSH S-transferase (GST, EC 2.5.1-18, from bovine liver; Sigma, 0.6 U/ml, 10 min before Atr). After addition of 10  $\mu$ l alkaline phosphatase (5 U/ml, Boehringer Mannheim) diluted in liposome buffer +0.5 mM  $MgCl_2$ , samples were incubated for 15 min at 37°C and the enzymatic conversion of 4-MUP to 4-MU (4-methylumbelliferone) was stopped by addition of 50  $\mu$ l stop buffer (10 mM HEPES-NaOH, 200 mM EDTA, pH 10.0). Fluorescence was subsequently determined using a Perkin Elmer spectrofluorimeter (excitation 365 nm, emission 450  $\pm$  5 nm).<sup>25</sup>

## Results and discussion

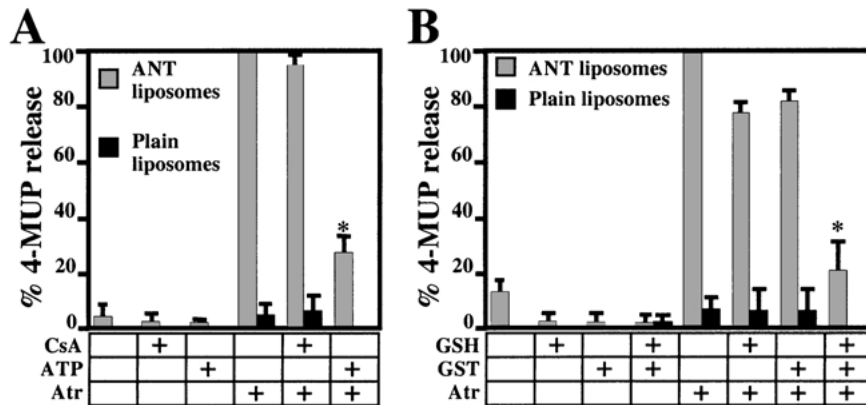
### *In vitro* Atr toxicity is modulated by CsA and GSH

Human hepatic cells cultured in the presence of Atr manifest a rapid cell death (2 hours) either by necrosis (defined by the uptake of the vital dye propidium iodine without manifest chromatin condensation detectable by Hoechst 33324) or by apoptosis (defined by chromatin condensation with or without loss of viability) (Figure 1A). This cytotoxic effect is strongly inhibited by CsA (Figure 1A and B) as well as by *N*-methyl-4-Val-CsA (m-CsA), a non-immunosuppressive CsA derivative which does not inhibit the calcineurin pathway, yet continues to bind to mitochondrial cyclophilin D and to inhibit MMP<sup>41</sup> (Figure 1B). Pre-incubation of cells with the thiol oxidizing agent diethylenemaleimide (DEM) or the GSH synthase inhibitor butylsulfoximide (BSO) enhanced the cytotoxic effect of Atr. Conversely, the GSH precursor *N*-acetylcysteine (NAC) and cell-permeable GSH ethyl ester reduced Atr toxicity. In conclusion, CsA and GSH counteract the cytotoxic action of Atr.

### Prevention of *in vitro* Atr toxicity involves MMP inhibition

Control hepatoma cells stained with the  $\Delta\Psi_m$ -sensitive dye JC-1 contain mitochondria with a high  $\Delta\Psi_m$ , as indicated by the cytoplasmic red fluorescence. In contrast, Atr-treated cells exhibited a red-green fluorescence shift indicative of a  $\Delta\Psi_m$  loss. This  $\Delta\Psi_m$  loss was attenuated (orange fluorescence) in CsA-treated cells (Figure 2A). Similarly, m-CsA, NAC, and GSH ethyl ester counteracted the  $\Delta\Psi_m$  loss, while DEM and BSO enhanced the Atr-induced  $\Delta\Psi_m$  dissipation (Figure 2B). Similar results were obtained when cells were fixed and permeabilized, followed by immunofluorescence detection of Cyt *c* or AIF. Atr caused the release of Cyt *c* and AIF from mitochondria, while CsA, m-CsA, NAC, and GSH ethyl ester largely prevented the translocation of Cyt *c* and AIF to an extramitochondrial localization (not

**Figure 3.** Modulation of Atr-induced permeabilization of ANT proteoliposomes. (A) Effect of cyclophilin D ligands. 4-MUP-loaded plain liposomes or ANT proteoliposomes were pre-incubated in the absence or presence of CsA or the physiological ANT ligand ATP, followed by exposure to Atr and determination of 4-MUP release, as detailed in materials and methods. (B) Effect of GSH and GST. 4-MUP-loaded plain liposomes or ANT proteoliposomes were pretreated with GSH and/or GST, followed by exposure to Atr and determination of liposomal membrane permeabilization. Results are representative of four different experiments.



shown). CsA must prevent Atr-induced MMP in an indirect fashion. Thus, it failed to prevent the Atr-induced permeabilization of ANT proteoliposomes induced *in vitro* (Figure 3A), presumably because such a system lacks the CsA target cyclophilin D.<sup>7,14,15,17</sup> In contrast, the combination of GSH and GST S-transferase (but neither of the two compounds alone) did inhibit the Atr-mediated permeabilization of ANT proteoliposomes (Figure 3B), in accord with the previously reported finding that thiol derivatization of ANT can counteract MMP.<sup>8</sup> In conclusion, both CsA and GSH prevent Atr-induced MMP through indirect and direct effects on the ANT, respectively.

#### Atr lethality is reduced by CsA and GSH *in vivo*

Injection of Atr into mice (300 mg/kg i.p.) is lethal within a few hours. Atr lethality is significantly postponed by a diet deficient in sulfur amino acids (SAA<sup>-</sup>) or enriched in such amino acids (SAA<sup>+</sup>), a regime which reduces or enhances the mitochondrial GSH content, respectively.<sup>36</sup> SAA<sup>-</sup> mice died more rapidly than control mice, whereas SAA<sup>+</sup> died later (Figure 4). Similarly, CsA administration significantly reduced the lethal effect of Atr *in vivo* (Figure 4). These observations could be correlated with the histopathological appearance of hepatic lobules and the renal cortex. Animals treated with Atr exhibited a cytoplasmic vacuolization, both in hepatocytes, whatever their exact localization in the hepatic lobule, and in proximal (but not distal) renal tubular cells (Figures 5 and 6). These changes were dramatically reduced by CsA treatment (Figures 5 and 6). The accumulation of cellular debris in the lumen of renal tubuli induced by Atr was also inhibited by CsA and SAA-rich diet (Figure 6).

As a result, it appears that CsA and GSH can reduce Atr toxicity *in vivo*.

#### CsA and GSH counteract Atr-induced MMP and cell death *in vivo*

Ultrastructural examination of hepatocytes or proximal tubuli from Atr treated mice did not reveal any apparent alteration in mitochondrial morphology (Figure 6), at difference of mice that have been treated with anti-CD95/Fas antibody.<sup>38</sup> Nonetheless, Atr triggered MMP *in vivo*, as shown by immunofluorescence staining with antibodies specific for AIF or cytochrome *c* (red fluorescence) and

**Figure 4.** Effects of CsA and GSH on Atr toxicity *in vivo*. Mice (20 animals per group), kept under a standard diet (Co.), a diet supplemented in SAA (SAA<sup>+</sup>) or an SAA-deficient diet (SAA<sup>-</sup>) were injected with Atr (300 mg per kg body weight), and survival was monitored each 6 to 12 hours. Alternatively, mice were pre-treated by intraperitoneal injection of CsA. CsA and the SAA<sup>+</sup> diet both significantly ( $p < 0.001$ ) prolonged survival, as compared to Atr-only treated control mice.

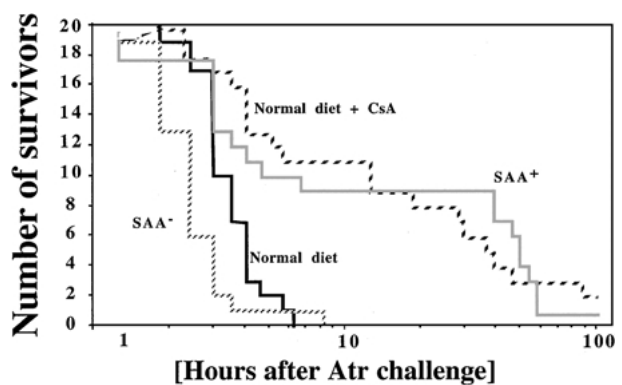


**Figure 5.** Histopathology of the liver (A–D) and the kidney (E–H) from mice injected with Atr alone (A, E) or mice pretreated with an SAA<sup>+</sup> diet (B, F), an SAA<sup>-</sup> diet (C, G), or CsA (D, H). In A, Atr induced in most hepatocytes, irrespective of their distribution in the hepatic lobule, cytoplasmic vacuolization, yet failed to induce apoptosis or necrosis at this time point (2 h after Atr injection as in Figure 4). While the number of vacuoles per cell seemed unaffected by SAA (B, C), CsA (D) reduced vacuolization, except for a few cells in the periportal area. Numerous vacuoles are also visible in many proximal tubular cells from mice receiving Atr alone (E), without that this parameter would be influenced by diet (F, G). Note that the tubular lumen is occupied by cell debris and that no apoptosis or necrosis is visible in tubular cells. Upon CsA pretreatment, most proximal tubules were left normal (fig. J). Original magnification 1 × 200.

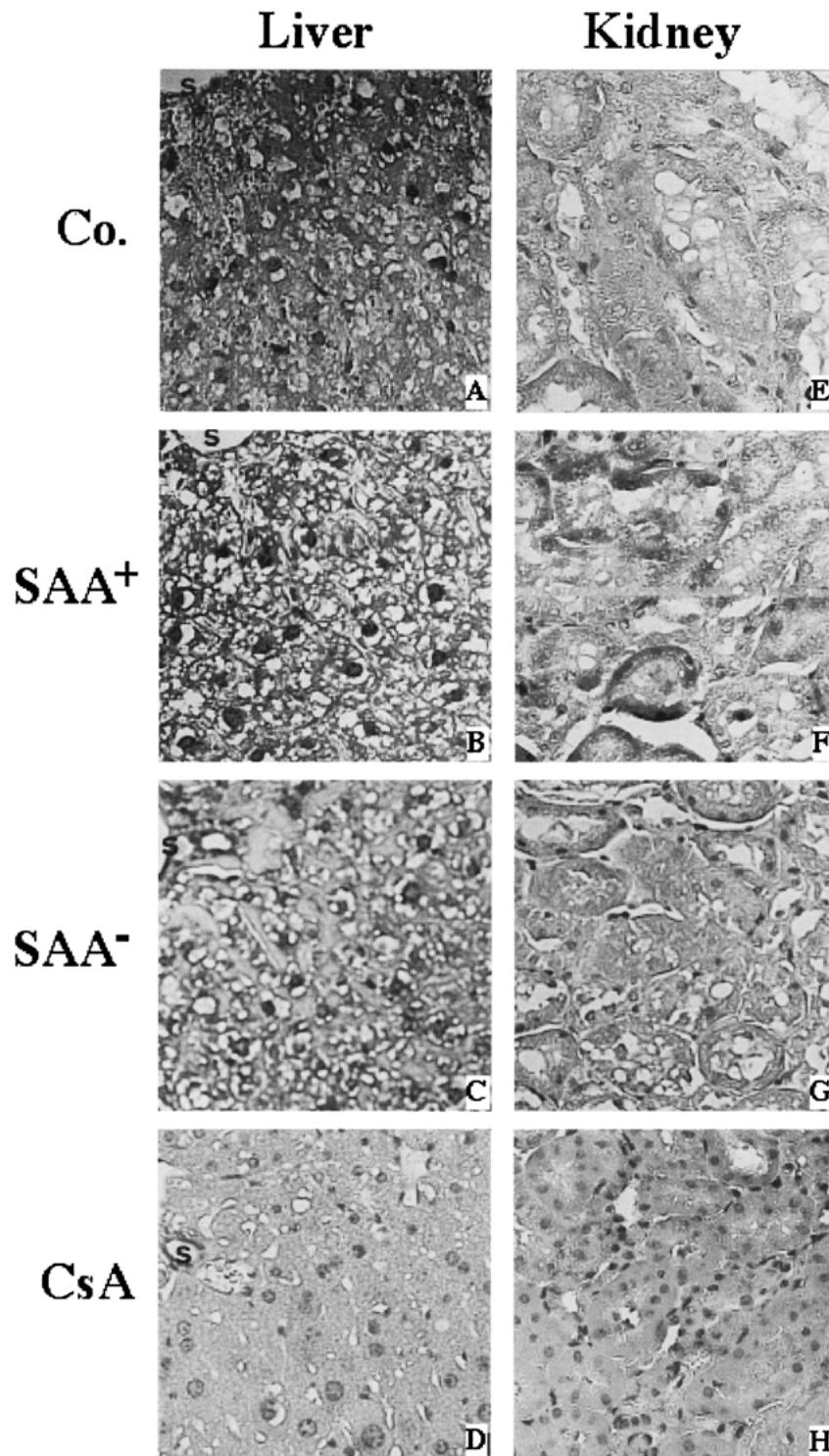


**Figure 6.** Ultrastructure of hepatocytes (A, B, C) and kidney tubular cells (D, E, F) from mice receiving Atr alone (A, D) or Atr in combination with CsA (B, E) or Atr plus SAA (C, F) (doses and treatment as in Figures 4 and 5). In A, voluminous vacuoles (V) are visible in the hepatocyte cytoplasm. The endoplasmic reticulum (ER) is disorganized and dilated while mitochondria (m) appear normal. In B, the appearance of the hepatocyte is almost normal with a minor disorganization of the ER. In C, vacuoles (V) and ER changes are still present but less marked than in A. Mitochondria (m) are also normal. In D, numerous small vesicles (v) are observed in the cytoplasm of tubular cells while mitochondria (m) appear normal. Note that microvilli (arrowheads) are altered and cell debris (asterisks) are visible in the tubular lumen. In E, this tubular cell is almost normal. In F, vacuoles (V) are visible in the cytoplasm of some tubular cells. N: Nucleus; L: Lumen. Original magnifications: A:  $\times 7400$ , B:  $\times 9000$ , C:  $\times 7400$ , D:  $\times 2900$ , E:  $\times 4900$ , F:  $\times 3400$ .

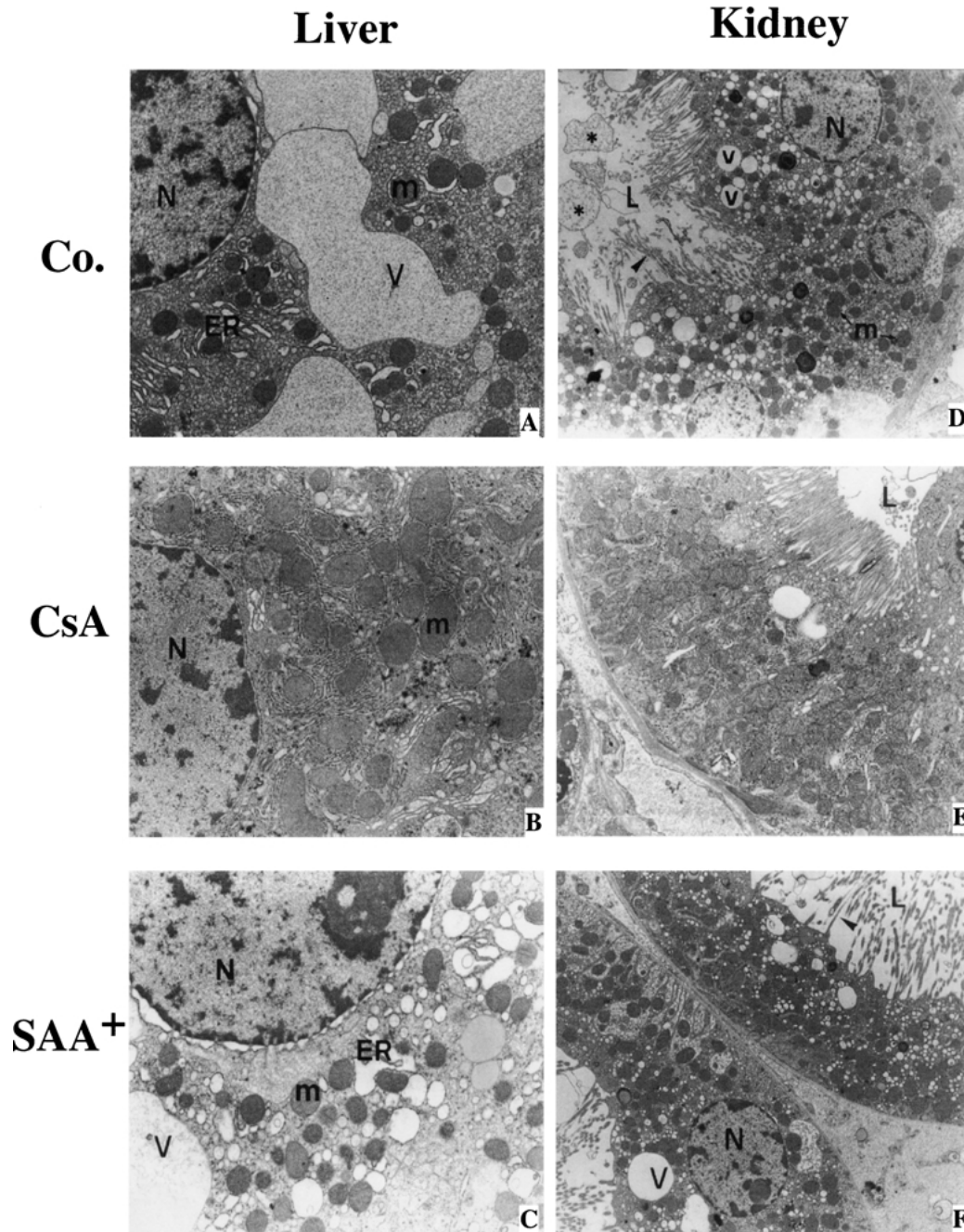
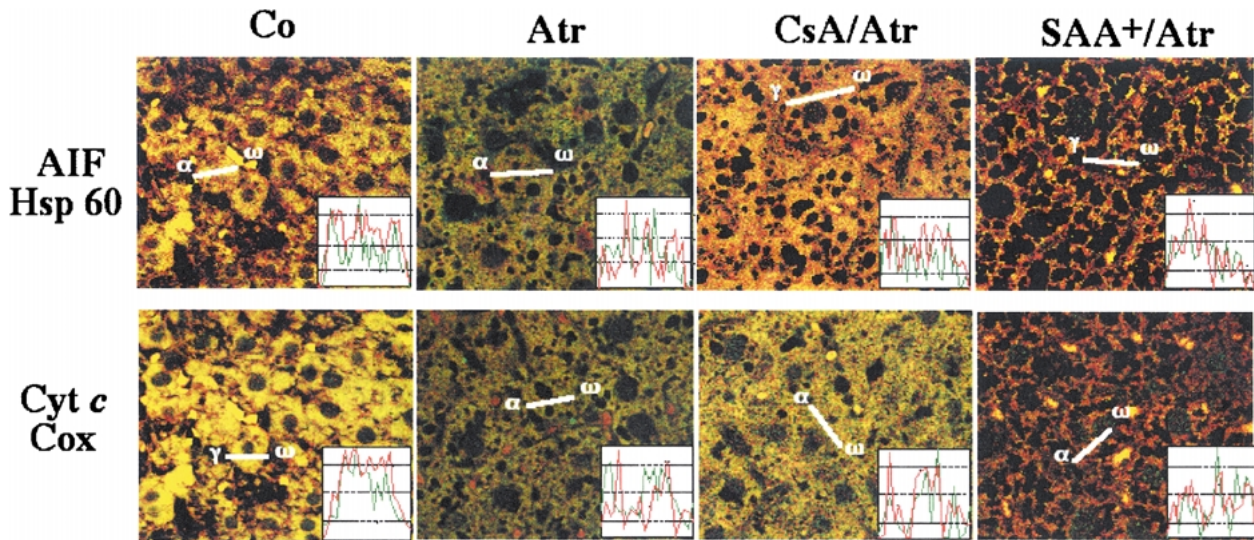


**Figure 7.** Apoptosis-associated release of AIF from mitochondria. Liver sections from mice receiving the indicated treatment were stained with antibodies specific for AIF (red fluorescence) and Hsp60 (green fluorescence) or were stained for Cyt *c* (red) and COX (green), and were analyzed by confocal microscopy. The fluorescence fusion image reflecting the dominant (>90%) phenotype of subcellular AIF distribution are shown for each treatment. The graphs (inserts) represent the fluorescence distribution of one representative section (orientation indicated by  $\alpha$  and  $\omega$ ). Note the colocalization (yellow color) of AIF and Hsp60 or Cyt *c* and COX in liver cells from untreated mice (Co.), which contrasts with the relative loss of AIF and Cyt *c* staining intensity (yellow  $\rightarrow$  green shift) in Atr-treated mice, as well as the differential distribution of the red and the green fluorescence (inserts). CsA and SAA supplementation reduced this Atr effect. Results are representative of >50 confocal sections from two different livers each.



counterstaining for sessile mitochondrial markers such as Hsp60 or COX (green fluorescence). Atr treatment did not affect the intensity and the subcellular distribution of Hsp60 and COX, yet caused an overall decrease in the AIF- or Cyt *c*-specific fluorescence (note the yellow-green shift), with a spatial separation of the red and the green fluorescence (see inserts) observable by confocal microscopy (Figure 7). This indicates that Atr triggered the mitochondrial release of AIF and Cyt *c*, thus confirming the finding reported by others<sup>42,43</sup> that MMP can occur without changes in mitochondrial ultrastructure. The Atr-induced changes in the subcellular distribution of AIF and Cyt *c* were attenuated by either CsA or an SAA<sup>+</sup> diet, the CsA effect being stronger than that of SAA supplementation. Similar results were obtained for hepatocytes (Figure 7) and renal cells (not shown). In conclusion, Atr induces MMP *in vivo*, and MMP interaction is reduced by CsA and GSH.

#### Acetaminophen lethality is reduced by CsA and GSH *in vitro* and *in vivo*

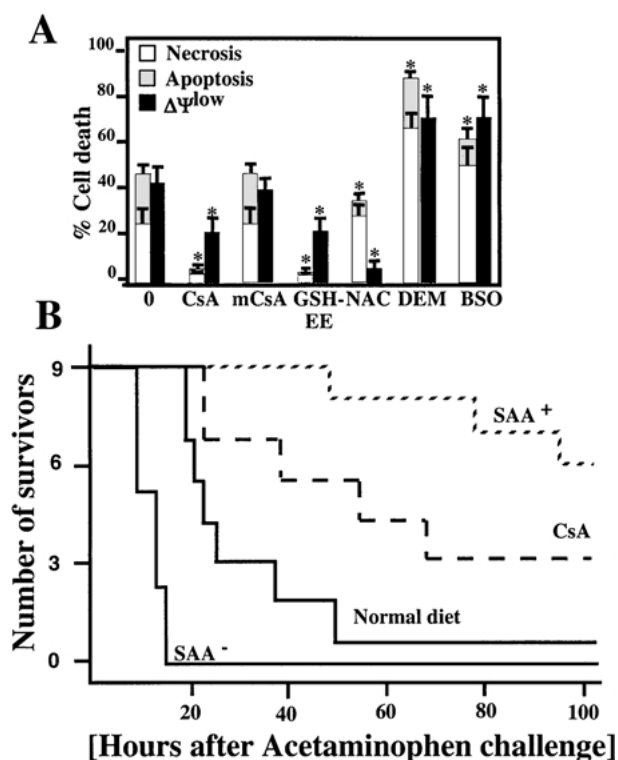
Although Atr is an interesting compound, based on its specificity for ANT, its relevance to human medicine is reduced, with as little as one hundred annual fatalities, mostly in North Africa.<sup>3</sup> We wondered whether a similar principle of lethal action might apply to a less specific hepatotoxic and renotoxic compound such as the analgesic acetaminophen (paracetamol).<sup>44-46</sup> Acetaminophen

added to human liver cells caused rapid (2 hours) cell death, and this effect was inhibited by CsA, m-CsA, N-acetylcysteine, and GSH ethyl ester. In contrast, two regimes of GSH depletion (DEM and BSO) enhanced the cytotoxic effect of acetaminophen (Figure 8A). Similar results were obtained *in vivo*, in a mouse model of acetaminophen toxicity. The lethal effect of acetaminophen injection was exacerbated by the SAA<sup>-</sup> diet and reduced, either by the SAA<sup>+</sup> diet or by continuous administration of CsA with an osmotic pump (Figure 8B). Thus, the mitochondrioprotective action of CsA and GSH can reduce the hepatorenal toxicity of acetaminophen.

#### Concluding remarks

As discussed in the introduction, Atr has two major effects on ANT, namely inhibition of the ATP/ADP antiporter (which, on theoretical grounds should lead to a cytosolic depletion of ATP generated by oxidative phosphorylation) and induction of PT with consequent MMP. The data shown here indicate that the MMP-inducing effect of Atr is determining its toxicity, given that CsA, which inhibits Atr-induced MMP (yet does not affect its antiporter function) can counteract the lethal effect of Atr. Moreover, although Atr has also been reported to cause the release of cathepsin B from lysosomes<sup>47</sup> and to inhibit the ryanodine receptor Ca<sup>2+</sup> channel in the sarcoplasmic reticulum,<sup>48</sup> such extramitochondrial effects apparently are not rate-limiting for its *in vitro* and *in vivo* toxicity. Indeed, it

**Figure 8.** CsA and GSH antagonize acute aminoacetophen toxicity *in vitro* and *in vivo*. (A) Cell death induction by aminoacetophen and its modulation in cultured liver cells. Cells were left untreated (Co.) or pretreated with CsA, m-CsA, or different GSH-modulating agents, which themselves do not affect cell viability or  $\Delta\Psi_m$  (Figures 1 and 2), followed by addition of aminoacetophen and determination of the percentage of cells with an apoptotic, necrotic or  $\Delta\Psi_m$  low phenotype. (B) Acute lethality of aminoacetophen *in vivo* and its modulation by CsA and SAA supplementation. Control mice, mice pretreated with an osmotic pump releasing CsA, or mice on SAA<sup>-</sup> or SAA<sup>+</sup> diet received an intraperitoneal injection of aminoacetophen, and survival was assessed. Similar results were obtained in two independent experiments.



appears that Atr has a direct membrane permeabilizing effect, either on purified mitochondria *in vitro*,<sup>34</sup> or on ANT proteoliposomes.<sup>13,26</sup>

Pharmacological evidence that ANT is critical for cell death induction is based on the fact that bongkreikic acid, an ANT ligand which inhibits both ANT functions (that is ATP/ADP antiport and pore formation),<sup>10</sup> can prevent cell death induced by a heterogeneous collection of stimuli including glucocorticoids,<sup>49</sup> pro-apoptotic members of the Bcl-2 family,<sup>13,50,51</sup> nitric oxide,<sup>52</sup> tumor necrosis factor- $\alpha$ ,<sup>53</sup> B cell receptor cross linking,<sup>54</sup> neurotoxins,<sup>55</sup> glutathione depletion,<sup>56</sup> bile acid,<sup>57</sup> staurosporin,<sup>58</sup> or hypoxia.<sup>59</sup> However, due to its intrinsic toxicity, bongkreikic acid cannot be administered in a systemic fashion and surrogate drugs indirectly impinging on the ANT-dependent MMP must be actively searched for. As shown here, CsA (and its non-immunosuppressive derivatives specifically targeted to cyclophilin D) provide a tool to evaluate the contribution of MMP to cytotoxic events *in vivo*

and, may perhaps, advance to a therapeutic agent of choice, whenever MMP mediates the toxicity of xenobiotics.

## Acknowledgments

This work has been supported by a special grant from the Ligue Nationale contre le Cancer, as well as grants from ANRS (to G.K.), FRM (to G.K. and C.B.), and the European Commission (QLG1-CT-1999-00739 to G.K.). H.L.A.V. receives a fellowship from the Fundação para a Ciência e a Tecnologia PRAXIS XXI, Portugal; P.B. from the European Commission (MCFI-2000-00943), I.C. and D.H. from the Ligue Nationale contre le Cancer, C. E. H. from the Comité Val de Marne de la Ligue contre le Cancer, A.-S.B. from Association pour la Recherche sur le Cancer, D.P. from the Académie Nationale de Médecine.

## References

1. Dehrmann FM, Bye SN, Dutton MF. The isolation of a storage organelle of atractyloside in *Callipeis laureola*. *J Ethnopharmacol* 1991; 34: 247–251.
2. Hatch RC, Jain AV, Weiss R, Clark JD. Toxicologic study of carboxyatractyloside (active principle in cocklebur—*Xanthium strumarium*) in rats treated with enzyme inducers and inhibitors and glutathione precursor and depletor. *Am J Vet Res* 1982; 43: 111–116.
3. Stewart MJ, Steenkamp V. The biochemistry and toxicity of atractyloside: A review. *Ther Drug Monit* 2000; 22: 641–649.
4. Obatomi DK, Blackburn RO, Bach PH. Effects of the calcium channel blocker verapamil and sulphydryl reducing agent dithiothreitol on atractyloside toxicity in precision-cut rat renal cortical and liver slices. *Food Chem Toxicol* 2001; 39: 1013–1021.
5. Roux P, Le Saux A, Fiore C, Schwimmer C, Dianoux AC, Trezeguet V, Vignais PV, Lauquin GJ, Brandolin G. Fluorometric titration of the mitochondrial ADP/ATP carrier protein in muscle homogenate with atractyloside derivatives. *Anal Biochem* 1996; 234: 31–37.
6. Majima E, Shinohara Y, Yamaguchi N, Hong YM, Terada H. Importance of loops of mitochondrial ADP/ATP carrier for its transport activity deduced from reactivities of its cysteine residues with the sulphydryl reagent eosin-5-maleimide. *Biochemistry* 1994; 33: 9530–9536.
7. Halestrap AP, Woodfield KY, Connern CP. Oxidative stress, thiol reagents, and membrane potential modulate the mitochondrial permeability transition by affecting nucleotide binding to the adenine nucleotide translocase. *J Biol Chem* 1997; 272: 3346–3354.
8. Costantini P, Belzacq A-S, Vieira HLA, Larochette N, de Pablo M, Zamzami N, Susin SA, Brenner C, Kroemer G. Oxidation of a critical thiol residue of the adenine nucleotide translocator enforces Bcl-2-independent permeability transition pore opening and apoptosis. *Oncogene* 2000; 19: 307–314.
9. Vieira HL, Haouzi D, El Hamel C, Belzacq AS, Brenner C, Kroemer G. Mitochondrial membrane permeabilization during apoptosis. Impact of the adenine nucleotide translocator. *Cell Death Differ* 2000; 7: 1146–1154.
10. Klingenberg M. The ADP-ATP translocation in mitochondria, a membrane potential controlled transport. *J Membrane Biol* 1980; 56: 97–105.

11. Marzo I, Brenner C, Zamzami N, Susin SA, Beutner G, Brdiczka D, Rémy R, Xie Z-H, Reed JC, Kroemer G. The permeability transition pore complex: A target for apoptosis regulation by caspases and Bcl-2 related proteins. *J Exp Med* 1998; 187: 1261–1271.
12. Beutner G, Rück A, Riede B, Welte W, Brdiczka D. Complexes between kinases, mitochondrial porin, and adenylate translocator in rat brain resemble the permeability transition pore. *FEBS Lett* 1996; 396: 189–195.
13. Marzo I, Brenner C, Zamzami N, Jürgensmeier J, Susin SA, Vieira HLA, Prévost M-C, Xie Z, Matsuyama S, Reed JC, Kroemer G. Bax and adenine nucleotide translocator cooperate in the mitochondrial control of apoptosis. *Science* 1998; 281: 2027–2031.
14. Crompton M, Virji S, Ward JM. Cyclophilin-D binds strongly to complexes of the voltage-dependent anion channel and the adenine nucleotide translocase to form the permeability transition pore. *Eur J Biochem* 1998; 258: 729–735.
15. Woodfield K, Ruck A, Brdiczka D, Halestrap AP. Direct demonstration of a specific interaction between cyclophilin-D and the adenine nucleotide translocase confirms their role in the mitochondrial permeability transition. *Biochem J* 1998; 336: 287–290.
16. Bauer MKA, Schubert A, Rocks O, Grimm S. Adenine nucleotide translocase-1, a component of the permeability transition pore, can dominantly induce apoptosis. *J Cell Biol* 1999; 147: 1493–1501.
17. Crompton M. Mitochondrial intermembrane junctional complexes and their role in cell death. *J Physiol* 2000; 15: 11–21.
18. Kroemer G, Reed JC. Mitochondrial control of cell death. *Nat Med* 2000; 6: 513–519.
19. Brustovetsky N, Klingenberg M. Mitochondrial ADP/ATP carrier can be reversibly converted into a large channel by  $Ca^{2+}$ . *Biochemistry* 1996; 35: 8483–8488.
20. Rück A, Dolder M, Wallimann T, Brdiczka D. Reconstituted adenine nucleotide translocator forms a channel for small molecules comparable to the mitochondrial permeability transition pore. *FEBS Lett* 1998; 426: 97–101.
21. Brenner C, Cadiou H, Vieira HLA, Zamzami N, Marzo I, Xie Z, Leber B, Andrews D, Duclouhier H, Reed JC, Kroemer G. Bcl-2 and Bax regulate the channel activity of the mitochondrial adenine nucleotide translocator. *Oncogene* 2000; 19: 329–336.
22. Kroemer G, Dallaporta B, Resche-Rigon M. The mitochondrial death/life regulator in apoptosis and necrosis. *Annu Rev Physiol* 1998; 60: 619–642.
23. Zamzami N, El Hamel C, Muñoz C, Brenner C, Belzacq A-S, Costantini P, Molle G, Kroemer G. Bid acts on the permeability transition pore complex to induce apoptosis. *Oncogene* 2000; 19: 6342–6350.
24. Jacotot E, Ferri KF, El Hamel C, Brenner C, Druillenc S, Hoebeke J, Rustin P, Métivier D, Lenoir C, Geuskens M, Vieira HLA, Loeffler M, Belzacq A-S, Briand J-P, Zamzami N, Edelman L, Xie ZH, Reed JC, Roques BP, Kroemer G. Control of mitochondrial membrane permeabilization by adenine nucleotide translocator interacting with HIV-1 Vpr and Bcl-2. *J Exp Med* 2001; 193: 509–520.
25. Vieira HL, Belzacq A-S, Haouzi D, Bernassola F, Cohen I, Jacotot E, Ferri KF, Hamel EH, Bartle LM, Melino G, Brenner C, Goldmacher V, Kroemer G. The adenine nucleotide translocator: A target of nitric oxide, peroxynitrite and 4-hydroxynonenal. *Oncogene* 2001; 20: 4305–4316.
26. Belzacq AS, El Hamel C, Vieira HLA, Cohen I, Haouzi D, Metivier D, Marchetti P, Goldmacher V, Brenner C, Kroemer G. The adenine nucleotide translocator mediates the mitochondrial membrane permeabilization induced by Ionidamine, arsenite and CD437. *Oncogene* 2001; 20: 7579–7587.
27. Fiore C, Tezeguet V, LeSaux A, Roux P, Schwimmer C, Dianoux AC, Noel F, Lauquin GJM, Brandolin G, Vignais PV. The mitochondrial ADP/ATP carrier: Structural, physiological and pathological aspects. *Biochimie* 1998; 80: 137–150.
28. Zoratti M, Szabò I. The mitochondrial permeability transition. *Biochem Biophys Acta - Rev Biomembranes* 1995; 1241: 139–176.
29. Bernardi P. The permeability transition pore. Control points of a cyclosporin A-sensitive mitochondrial channel involved in cell death. *Biochim Biophys Acta (Bioenergetics)* 1996; 1275: 5–9.
30. Petit PX, Gubern M, Diolez P, Susin SA, Zamzami N, Kroemer G. Disruption of the outer mitochondrial membrane as a result of mitochondrial swelling. The impact of irreversible permeability transition. *FEBS Lett* 1998; 426: 111–116.
31. Quin ZH, Wang Y, Kikly KK, Sapp E, Kegel KB, Aronin N, DiFiglia M. Pro-caspase-8 is pre-dominantly localized in mitochondria and released into cytoplasm upon apoptotic stimulation. *J Biol Chem* 2001; 276: 8079–8086.
32. Susin SA, Lorenzo HK, Zamzami N, Marzo I, Larochette N, Alzari PM, Kroemer G. Mitochondrial release of caspases-2 and -9 during the apoptotic process. *J Exp Med* 1999; 189: 381–394.
33. Susin SA, Lorenzo HK, Zamzami N, Marzo I, Snow BE, Brothers GM, Mangion J, Jacotot E, Costantini P, Loeffler M, Larochette N, Goodlett DR, Aebersold R, Siderovski DP, Penninger JM, Kroemer G. Molecular characterization of mitochondrial apoptosis-inducing factor. *Nature* 1999; 397: 441–446.
34. Zamzami N, Susin SA, Marchetti P, Hirsch T, Gómez-Monterrey I, Castedo M, Kroemer G. Mitochondrial control of nuclear apoptosis. *J Exp Med* 1996; 183: 1533–1544.
35. Susin SA, Zamzami N, Castedo M, Hirsch T, Marchetti P, Macho A, Daugas E, Geuskens M, Kroemer G. Bcl-2 inhibits the mitochondrial release of an apoptogenic protease. *J Exp Med* 1996; 184: 1331–1342.
36. Haouzi D, Lekethal M, Tinel M, Vadrot N, Caussanel L, Letteron P, Moreau A, Feldmann G, Fau D, Pessayre D. Prolonged, but not acute, glutathione depletion promotes Fas-mediated mitochondrial permeability transition and apoptosis *in vivo*. *Hepatology* 2001; 33: 1181–1188.
37. Bump EA, Taylor YC, Brown JM. Role of glutathione in the hypoxic cell cytotoxicity of misonidasole. *Cancer Res* 1983; 43: 997–1002.
38. Feldmann G, Haouzi D, Moreai A, Durand-Schneider AM, Bringuier A, Berson A, Mansouri A, Fau D, Pessayre D. Opening of the mitochondrial permeability transition pore causes matrix expansion and outer membrane rupture in Fas-mediated hepatic apoptosis in mice. *Hepatology* 2000; 31: 674–683.
39. Daugas E, Susin SA, Zamzami N, Ferri K, Irinopoulos T, Larochette N, Prevost MC, Leber B, Andrews D, Penninger J, Kroemer G. Mitochondrio-nuclear redistribution of AIF in apoptosis and necrosis. *FASEB J* 2000; 14: 729–739.
40. Ferri KF, Jacotot E, Blanco J, Esté JA, Zamzami A, Susin SA, Brothers G, Reed JC, Penninger JM, Kroemer G. Apoptosis control in syncytia induced by the HIV-1-envelope glycoprotein complex. Role of mitochondria and caspases. *J Exp Med* 2000; 192: 1081–1092.
41. Khaspekov L, Friberg H, Halestrap A, Viktorov I, Wieloch T. Cyclosporin A and its nonimmunosuppressive analogue N-Me-Val-4-cyclosporin A mitigate glucose/oxygen deprivation-induced damage to rat cultured hippocampal neurons. *Eur J Neurosci* 1999; 11: 3194–3198.
42. Martinou I, Desagher S, Eskes R, Antonsson B, Andre E, Fakan S, Martinou JC. The release of cytochrome *c* from mitochondria

- during apoptosis of NGF-deprived sympathetic neurons is a reversible event. *J Cell Biol* 1999; 144: 883–889.
43. von Ahsen O, Renken C, Prkins G, Kluck RM, Bossy-Wetzell E, Newmeyer DD. Preservation of mitochondrial structure and function after Bid- or Bax-mediated cytochrome *c* release. *J Cell Biol* 2000; 150: 1027–1036.
  44. Prescott LF. Paracetamol: Past, present, and future. *Am J Ther* 2000; 7: 143–147.
  45. Rocha GM, Michea LF, Peters EM, Kirby M, Xu Y, Ferguson DR, Burg MB. Direct toxicity of nonsteroidal antiinflammatory drugs for renal medullary cells, 2001.
  46. Chan K, Han XD, Kan YW. An important function of Nrf2 in combating oxidative stress: Detoxification of acetaminophen. *Proc Natl Acad Sci USA* 2001; 98: 4611–4616.
  47. Vancompernelle K, Van Herreweghe F, Pynaert G, Van de Craen M, De Vos K, Totty N, Sterling A, Fiers W, Vandenabeele P, Grooten J. Atractyloside-induced release of cathepsin B, a protease with caspase-processing activity. *FEBS Lett* 1998; 6: 150–158.
  48. Yamaguchi N, Kagari T, Kasai M. Inhibition of the ryanodine receptor channels in the sarcoplasmic reticulum of skeletal muscle by an ADP/ATP translocase inhibitor, atractyloside. *Biochem Biophys Res Commun* 1999; 258: 247–251.
  49. Marchetti P, Castedo M, Susin SA, Zamzami N, Hirsch T, Haeflner A, Hirsch F, Geuskens M, Kroemer G. Mitochondrial permeability transition is a central coordinating event of apoptosis. *J Exp Med* 1996; 184: 1155–1160.
  50. Narita M, Shimizu S, Ito T, Chittenden T, Lutz RJ, Matsuda H, Tsujimoto Y. Bax interacts with the permeability transition pore to induce permeability transition and cytochrome *c* release in isolated mitochondria. *Proc Natl Acad Sci USA*, 1998; 95: 14681–14686.
  51. Vande Velde C, Cizeau J, Dubik D, Alimonti J, Brown T, Israels S, Hakem R, Greenberg AH. BIP3 and genetic control of necrosis-like cell death through the mitochondrial permeability transition pore. *Mol Cell Biol* 2000; 20: 5454–5468.
  52. Hortelano S, Dallaporta B, Zamzami N, Hirsch T, Susin SA, Marzo I, Bosca L, Kroemer G. Nitric oxide induces apoptosis via triggering mitochondrial permeability transition. *FEBS Lett* 1997; 410: 373–377.
  53. Hehner SP, Hofmann TG, Ratter F, Dumont A, Dröge W, Schmitz ML. Tumor necrosis factor-alpha induced cell killing and activation of transcription factor NF-kappa B are uncoupled in L929 cells. *J Biol Chem* 1998; 273: 18117–18121.
  54. Doi T, Motoyama N, Tokunaga A, Watanabe T. Death signals from the B cell antigen receptor target mitochondria, activating necrotic and apoptotic death cascades in a murine B cell line, WEHI-231. *Int Immunol* 1999; 11: 933–941.
  55. Budd SL, Tenneti L, Lishnak T, Lipton SA. Mitochondrial and extramitochondrial apoptotic signaling pathways in cerebrocortical neurons. *Proc Natl Acad Sci USA* 2000; 97: 6161–6166.
  56. O'Neill AJ, O'Neill S, Hegarty NJ, Coffey RN, Gibbons N, Brady H, Fitzpatrick JM, Watson RW. Glutathione depletion-induced neutrophil apoptosis is caspase 3 dependent. *Shock* 2000; 14: 605–609.
  57. Yerushalmi B, Dahl R, Devereaux MW, Gumprich E, Sokol RJ. Bile acid-induced rat hepatocyte apoptosis is inhibited by antioxidants and blockers of the mitochondrial permeability transition. *Hepatology* 2001; 33: 616–626.
  58. Tafani M, Minchenko DA, Serroni A, Farber JL. Induction of the mitochondrial permeability transition mediates the killing of HeLa cells by staurosporine. *Cancer Res* 2001; 61: 2459–2466.
  59. Gurevich RM, Regula KM, Kirshenbaum LA. Serpin protein CrmA suppresses hypoxia-mediated apoptosis of ventricular myocytes. *Circulation* 2001; 103: 1984–1991.